Influence of parameters in vapour transport equilibration treatment on composition and homogeneity of $LiTaO_3$ single crystals

*Minerva Gonzalez, Samuel Margueron, Tomas Murauskas, Pascal Boulet, Ludovic Gauthier-Manuel, Bernard Dulmet, and Ausrine Bartasyte**

M. Gonzalez, T. Murauskas, S. Margueron, L. Gauthier-Manuel, B. Dulmet, A. Bartasyte
FEMTO-ST Institute, University of Franche-Comté, CNRS (UMR 6174), ENSMM, Besançon, France
E-mail: ausrine.bartasyte@femto-st.fr

P. Boulet
Jean Lamour Institute, CNRS (UMR 7198), University of Lorraine, Nancy, France

A. Bartasyte
Institut Universitaire de France, Paris, France

Keywords: $LiTaO_3$ single crystals, vapor transport equilibration, Li stoichiometry, Raman spectroscopy

The effect of key parameters such as time, temperature, and equilibration powder concentration in vapour transport equilibration treatment on the Li_2O content of initially congruent X-, Y- and Z-cut $LiTaO_3$ crystals is experimentally investigated. The Li_2O content across the thickness of the crystal is estimated by Raman spectroscopy with accuracy of 0.05-0.15 mol%. The Li_2O loss from equilibration powders has been monitored as a function of treatment temperature and duration. The results show that the Li_2O content in the crystal nonlinearly depends on the equilibration powder composition and that homogeneous stoichiometric $LiTaO_3$ crystals can be obtained by treatment for at least 36h at 1250 °C in Li_2O rich atmosphere, created by powders containing > 54 mol% of Li_2O. The anisotropic Li^+ diffusion coefficients and its activation energy are also experimentally estimated. Finally, the vapour transport equilibration conditions are defined for production of different cuts of $LiTaO_3$ crystals with controlled homogeneous Li_2O nonstoichiometry in the range from sub-congruent to stoichiometric compositions.

1. Introduction

$LiNbO_3$ (LN) and $LiTaO_3$ (LT) single crystals are highly used in piezoelectric, pyroelectric, acousto-optic, non-linear optical and surface acoustic wave (SAW) devices. For example, the most of radio frequency (RF) SAW filters are fabricated from LT and LN single crystals, due to their piezoelectric properties such as good electromechanical coupling factor (K^2= 7-10%) [1]. The most available commercially LN and LT crystals are produced by Czochralski method, have a congruent composition (48.38 mol% and 48.5 mol%, respectively) and possesses many intrinsic defects. However, LN and LT phase can exist in a wide range of composition (46.5 – 50 mol% of Li_2O) [2,3]. Non-stoichiometry of Li_2O highly affects the structural and physical properties of LN and LT such as lattice parameters [2], Curie temperature (T_c) [4], [5], birefringence[6] and ferroelectric properties. Stoichiometric crystals exhibits less defects [7] than the congruent crystals, which reduce undesirable effects in optics [8]–[10]. Moreover, LT crystals with 49.3 mol% of Li_2O present zero birefringence at room temperature [11, 12]. The elastic properties and the acoustic performance including electromechanical coupling factor, temperature coefficient of frequency and wave propagation velocity are also dependent on the Li nonstoichiometry [13, 14]. Besides, SLT and SLN have a coercive field strength 100 times smaller than congruent crystal, which facilitates its ferroelectric domain reversal [15–17]. LN and LT crystals with sub-congruent compositions should offer better stability of acoustic filters at high power densities thanks to their higher coercive fields than that of congruent crystals.

Li is a light element, and then its concentration cannot be very precisely estimated by using directs methods. Several indirect methods have been proposed for example, measurement of UV absorption edges (with an accuracy of 0.05 mol%)[18], birefringence (0.1 mol%)[19-21], Curie temperature (0.1 mol%) [5,22], lattice parameters by X-ray diffraction (XRD, precision of 0.4 mol%) [2,22,23], and Raman mode dampings [20,21,24]. In this last technique, Li_2O concentration can be determined by accurate measurement (± 0.05 mol%) of Raman mode damping parameters (FWHM) of phonon bands due to their linear dependence on defect concentration [21].

In order to obtain stoichiometric or nearly-stoichiometric crystals, several techniques have been developed without reaching industrial application maturity. For example the double crucible Czochralski (DCCZ) method [25,26] or the top-seeded solution growth (TSSG) with K_2O quasi-flux [27–29]. An alternative method is the vapor transport equilibration (VTE) [4,5,30,31]. This technique is a treatment of the congruent LT or LN single crystal wafers grown by standard Czochralski technique, realized at high temperature in an atmosphere with controlled partial Li_2O vapor pressure. In VTE processing, a Li-rich or Li-poor atmosphere at

high temperature surrounds the congruent crystal. It allows diffusion of Li_2O from the equilibration powder into the crystal through vapor phase or vice versa. The Li_2O content in crystal varies with time, temperature and initial concentration of equilibration powders. Most of studies of VTE process were carried out for LN crystals [4, 30,32–38]. In these works the study of influence of crystal cut and thickness of crystal on VTE treatment was done and the dependence of time and temperature of VTE for LN was also investigated. However, in the case of LT crystals, knowledge about VTE conditions is not exhaustive [5,40,41]. Recently a modified VTE process, named vapor transport infiltration (VTI), consisting of Li in-difusion at low temperature and composition homogenisation at higher temperature, was proposed [42]. It was demonstrated, that VTI enables to produce homogenous LT crystals with stoichiometric composition. However, there are no published works about detailed optimization of the parameters in VTE process, required to produce homogeneous crystals with different Li compositions varying from stoichiometric (SLT) to other compositions in the composition range LT phase existence (47 – 50 mol%). Thus, the present work focuses on these points. The diffusion dependence on the LT crystal orientation and VTE temperature was investigated. Effort was done to optimise the VTE conditions as temperature, duration and equilibration powder composition for controlled VTE process enabling the fabrication of crystals with controlled homogeneous composition in the crystal volume. Additionally, the ability of the equilibration powders with different compositions to deliver the Li_2O vapor and its change with time were studied.

2. Results and discussion

Crystals with a surface of 5x20 mm^2 and a thickness of 500 µm were treated by VTE in a Li-rich/Li-poor atmosphere created by an equilibration powder in a closed double crucible of alumina (Al_2O_3). The crucible arrangement is shown in **Figure 1**, half of the crucible volume was filled up by the equilibration powder.

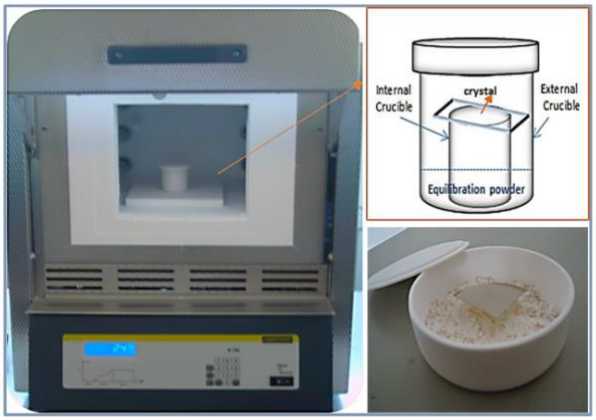

Figure 1. Schematic representation and photos of the experimental set-up used for VTE process. Alumina crucible had diameter of 115 mm and the height of 22 mm.

2.1. Composition study of equilibration powders

Single phase $Li_{1-x}Ta_{1+x}O_{3+2x}$ (hereafter $LT_{(1-x)/2}$) exists in the compositional range with Li_2O concentration, c_{Li2O}, from 47 mol% to 50 mol% [23]. In the composition range 25 mol% < c_{Li2O} < 47 mol%, $Li_{0.94}Ta_{1.06}O_{3.12}$ ($LT_{0.47}$) coexists with $LiTa_3O_8$ (LT3), while composition range 50 mol% < c_{Li2O} < 75 mol% consists of stoichiometric $LiTaO_3$ ($LT_{0.5}$) and Li_3TaO_4 (L3T) phases. Initially for the calibration purposes, the composition of synthesized equilibration powders was assumed to be the same as the molar ratio of Li:Ta in the initial mixture of Li_2CO_3 and Ta_2O_5 powders [12]. The change of a- and c-lattice parameters (estimated from XRD data, [12, 23]) was calibrated as a function of molar percentage of Li_2O in the powders, X_{Li2O} (**Figure 2 a**). For easier differentiation, the Li_2O concentration within the equilibration powders and the crystals will be named X_{Li2O} and C_{Li2O}, respectively. In the single-phase $Li_{1-x}Ta_{1+x}O_{3+2x}$ region, both a- and c-lattice parameters of the standard hexagonal unit cell decreases identically and linearly with the increase of the Li content up to the stoichiometric composition:

$$c = 13.882 - 0.002X_{Li2O} \text{ and} \quad (1)$$

$$a = 5.236 - 0.002X_{Li2O}. \quad (2)$$

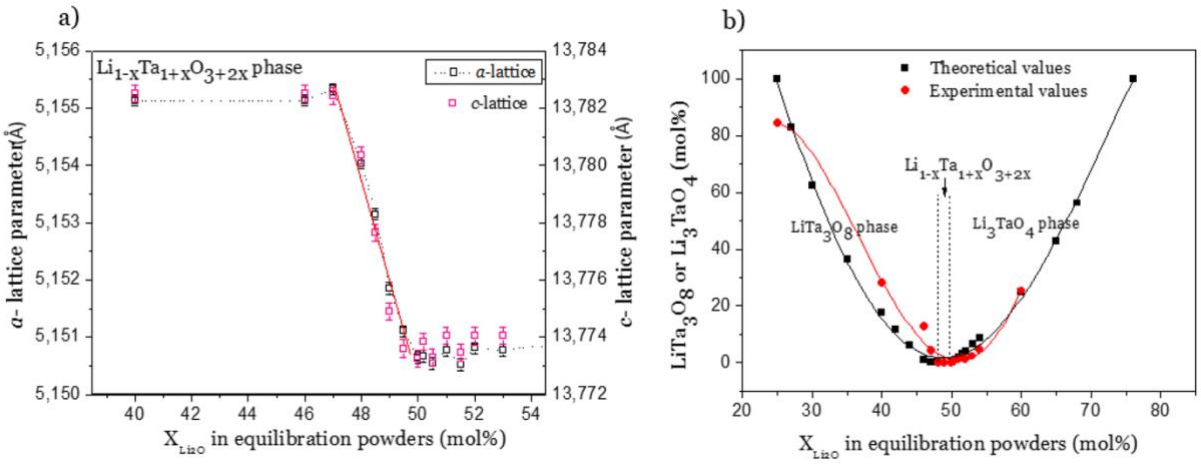

Figure 2. Change of a- and c-lattice parameters as a function of molar percentage of Li_2O in the single-phase and two-phase Li_2O-Ta_2O_5 solutions (a). Comparison of molar percentage of $LiTa_3O_8$ or Li_3TaO_4 phase, estimated theoretically and from XRD data, in the powders with different Li_2O composition in the range from 25 mol% to 75 mol% (b).

Raman spectroscopy was used as an alternative method for the composition analysis of the single-phase $LT_{(1-x)/2}$ powders. The Raman modes were identified according to the assignment given in Ref. [43]. For this purpose, the damping parameters (full width at half maximum, FWHM) of A_1(4TO) mode in unpolarized Raman spectra as a function of Li_2O content in

powders were studied. Similarly to the XRD data, a linear relationship between FWHM and X_{Li2O} was found:

$$X_{Li2O} = 55.16 - 0.41FWHM. \quad (3)$$

In the following experiments the composition of synthetized single-phase equilibration powders was systematically checked before and after VTE process by XRD and Raman spectroscopy and in general, very good agreement (in the range of the errors) between values estimated by these two alternative methods was obtained as illustrated in the **Table 1**.

Table 1. Comparison of X_{Li2O} (mol%) in equilibration powders, as expected from initial Li:Ta ratio in the starting powders and those estimated by means of XRD from c-lattice parameter (**Equation 1**) and by means of Raman Spectroscopy (**Equation 3**).

Expected X_{Li2O}	Measured X_{Li2O}	
	XRD (± 0.2 mol%)	Raman (± 0.05 mol%)
47.0	47.3	47.17
49.0	49.1	49.20
49.5	49.9	49.81
50.0	50.1	49.93

The $Li_{0.94}Ta_{1.06}O_{3.12}$ ($LT_{0.47}$) and $LiTaO_3$ ($LT_{0.5}$) compositions remain stable in the Li-poor and Li-rich two-phase composition regions, therefore their lattice parameters and damping of Raman modes do not change with further decrease/increase Li_2O content, which is compensated by the increasing molar ratio of the LT3 and L3T phase in the mixture, respectively. To study the composition of two-phase powders, the molar percentage of the secondary phase (LT3 or L3T) was quantified from XRD Θ/2Θ patterns by means of Rietveld refinement. The molar percentage of LT3 and L3T phases in Li-poor and Li-rich two-phase powders was estimated by equilibrating these chemical reactions:

$A\ Li_2O + B\ Ta_2O_5 \Rightarrow C Li_{0.94}Ta_{1.06}O_{3.12} + D\ LiTa_3O_8$ for $X_{Li2O} < 47$ mol% and (4)

$F\ Li_2O + G\ Ta_2O_5 \Rightarrow H\ LiTaO_3 + I\ Li_3TaO_4$ for $X_{Li2O} > 50$ mol%, respectively. (5)

The comparison of the theoretically expected and experimentally estimated from XRD data LT3 and L3T phase molar ratios in the two-component powder is given in **Figure 2 b**. One can also note that the secondary phase percentage increases nonlinearly with the change of Li_2O content. The theoretical dependence (**Figure 2 b**) was used to estimate the Li_2O amount in the equilibration two-phase powders before and after VTE process. The estimation error was estimated to be of 5 mol% according to the deviation of the experimentally estimated concentrations from the theoretical ones (**Figure 2 b**).

2.2. Li_2O loss in powders during VTE process

Li_2O partial pressure is the key parameter in VTE process defining the homogeneity and the composition of treated LT crystal. In most of previous works the VTE process was assumed to be equilibrium process with constant Li_2O vapor pressure. However, if the used crucible is not completely hermetically closed and/or the crucible is made of ceramics (like in the set-up used in this work, Figure 1), the Li_2O oxide escapes from the VTE environment and the powders continuously change their composition. Therefore, the change of equilibration powder composition as a function of time was studied at two VTE temperatures 1250 °C and 1300 °C. For this purpose, the initial equilibration powder with X_{Li2O} = 60 mol%, was treated sequentially at VTE temperature and its composition was checked after each treatment by means of Raman spectroscopy and/or XRD (see above). The change of equilibration powder composition as a function of time at 1250 °C and 1300 °C is presented in **Figure 3 a**. In the case of L3T and $LT_{0.5}$ phase mixture (X_{Li2O} > 50 mol %), the powder looses 0.17 mol%/h of Li_2O at 1300 °C and 0.02 mol%/h at 1250 °C, indicating a very strong dependence of VTE process on the temperature. This Li_2O loss can be attributed to the decomposition of L3T phase to $LT_{0.5}$ and Li_2O as the LT phase remains stoichiometric up to the single-phase region in the phase diagram. This decomposition is very fast at 1300 °C and the equilibration powder changes from 60 mol% of Li_2O to < 50 mol% in less than 60h, while it requires about 500h at 1250 °C. The single-phase $LT_{(1-x)/2}$ powders loose considerably less of Li_2O as compared to the powders containing L3T phase. Furthermore, the series of equilibration powders were synthesized and VTE treated for 24h at 1250 °C and 1300 °C. The total molar percentage of lost Li_2O during this duration as a function of the initial composition of the equilibration powder is presented in **Figure 3 b**. Li_2O loss decreases from 14 mol%/24h for X_{Li2O} = 60 mol% to 5 mol%/24h for LT0.5 at 1300 °C, while it is < 1 mol%/24h at 1250 °C. The loss of Li_2O quickly decreases also in the LT phase with the increase of its nonstoichiometry. Although, the important Li_2O vapor pressure can be generated at 1300 °C, the powder composition is changing very fast, which makes possible only very short VTE processes and this makes the composition control challenging.

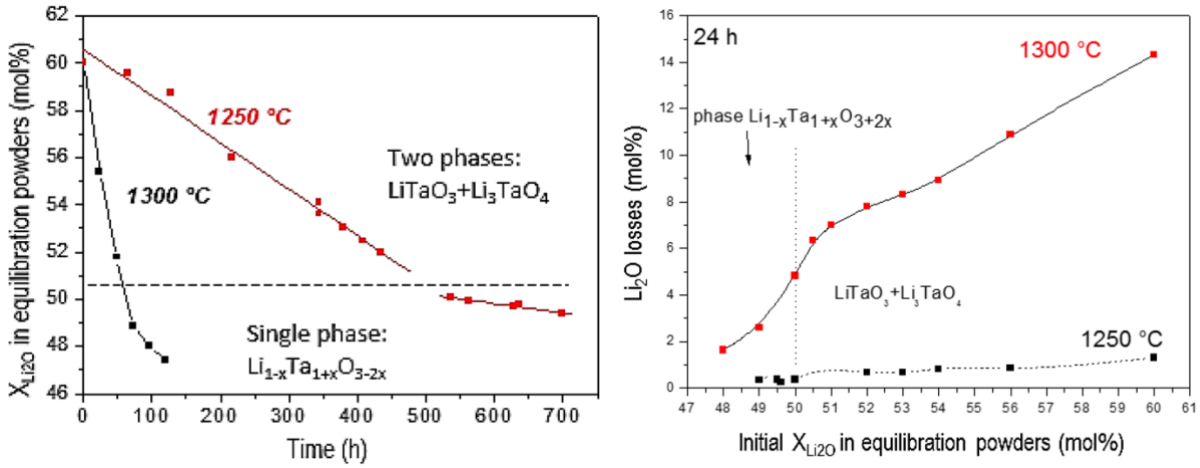

Figure 3. Composition change of equilibration powder (starting composition of powder X_{Li2O} = 60 mol%) as a function of time during VTE at 1250 °C and 1300 °C (a). Li_2O loss (in mol%) per 24h of VTE treatment at 1250 °C and 1300 °C as a function of initial equilibration powder composition (b).

2.3. Effect of VTE temperature on crystal concentration

For the study of VTE temperature effect, X-, Y- and Z-cut LT crystals were treated with equilibration powders with 40, 50 and 60 mol% of Li_2O for 10h at 1150 °C, 1200 °C, 1250 °C and 1300 °C. Short VTE duration (10h) was used to limit the effect of the change of the equilibration powder concentration with time and to decouple it from the studied effect of the VTE temperature. Li_2O concentration profile in the thickness of the crystal was estimated by measuring Raman spectra on the polished cross section of diced LT crystals after VTE treatment. Li_2O concentration in the cross-section of treated crystals was estimated from damping parameters (FWHM) of E(1TO) and E(7TO) modes in Raman spectra, measured in crossed polarization configuration:

C_{Li2O}(± 0.15 %mol)= 54.505 - 0.492$FWHM_{E(7TO)}$ for X- and Y-cut LT and (6)

C_{Li2O} (± 0.06 %mol)54.247 - 0.591$FWHM_{E(1TO)}$ for Z-cut LT. (7)

The polarization configurations used for the study of cross sections of different LT cuts were $Z(XY)\bar{Z}$ for X- and Y-oriented crystals and $Y(ZX)\bar{Y}$ for Z-orientation. The concentration profiles across the thickness of X-, Y-, and Z-LT crystal, treated by VTE at different temperatures by using equilibration powders with 40 mol%, 50 mol% and 60 mol% of Li_2O for 10 h are presented in **Figure 4**.

The Li_2O concentration on the treated X-, Y- and Z-LT crystal was also estimated on the crystal surface (few μm depth), C_s, by measuring polarized Raman spectra on the crystal surface ($X(YZ)\bar{X}$, $Y(ZX)\bar{Y}$, and $Z(XY)\bar{Z}$ polarization configurations, respectively). For this purpose, the E(1TO) and E(7TO) mode damping parameters (FWHM) were analysed:

C_{Li2O}(± 0.06 %mol)= 53.785 - 0.473$FWHM_{E(1TO)}$ for X- and Y-cut LT and (8)

$C_{Li2O}(\pm 0.15\ \%mol) = 54.247 - 0.591FWHM_{E(7TO)}$ for Z-cut LT. (9)

Then, ΔC_{Li2O} - the difference between the Li_2O concentration on the crystal surface (C_s) and that in the depth of 250 μm (in the middle of the crystal thickness, C_m) was evaluated:

$\Delta C_{Li2O} = C_s - C_m$. (10)

The ΔC_{Li2O}, $\bar{c}$ (average concentration across the crystal thickness), and C_s (concentration on crystal surface) of X-, Y-, and Z-cut crystals treated at different VTE temperatures are summarized in **Table 2**. The crystals treated in the temperature range from 1150 °C to 1250 °C present the Li_2O concentration gradient in the crystal thickness. The crystals treated at 1300 °C by using equilibration powders with $X_{Li2O} \geq 50$ mol% present almost homogenous Li_2O concentration across the crystals thanks to the significant Li_2O loss from equilibration powders and very fast Li^+ diffusion rates at 1300 °C. One can note that, Z-cut crystals in this case are homogenous while still small gradient can be observed in X- and Y- oriented crystals indicating that Li^+ diffusion is anisotropic and faster along Z-axis than those along X- and Y-axes.

The surface of the crystals treated by using Li-rich powders (60 mol% of Li_2O) presents nearly stoichiometric composition and the average crystal c_{Li2O} concentration approaches the stoichiometric one and the concentration gradient decreases with the increase of the VTE temperature. One can note that the Z-cut crystals present homogeneous stoichiometric composition after the VTE treatment at 1300 °C for 10h, while still small gradient exists in X- and Y-cut crystals treated at the same conditions. Temperatures lower than 1300 °C resulted in the concentration gradient across the thickness in all studied LT cuts. The gradient decreases and the Li_2O concentration in the central part of the thickness gradually increases from congruent to the stoichiometric one with the increase of VTE process temperature (Figure 4). The crystals treated at 1150 °C presented the Li concentration change in the depth of about 150 μm and the centre of the thickness presented unchanged composition (48.5 mol%). At higher temperatures (1300°C), the distribution of Li content becomes more homogenous in the crystals because the volatility and concentration of Li_2O vapor in powders depends strongly on treatment temperature, which agrees with results reported in literature [37,39]. It is important to note that these crystals presented very strong gradient, which induced in the thermal stresses during cooling down and resulted in the formation of twins [21].

The equilibration powders with X_{Li2O} = 50 mol% generate lower Li_2O partial vapor pressure with respect to the powders with 60 mol% of Li_2O. Thus, the X-, Y-, and Z-crystals treated at 1300 °C present homogeneous but nonstoichiometric composition with slightly increased Li_2O concentration with respect to the congruent composition (48.71 mol%, 48.54 mol%, and 48.66 mol%, respectively). The crystals treated at 1200 °C - 1250 °C present concentration gradients

and average Li_2O composition close to 49 mol%. In this case, the VTE treatment at 1150 °C resulted in the crystals with nearly stoichiometric composition on the surface (Table 2) which can be explained by the saturation of the Li concentration on the surface due to low diffusion to the crystal volume. The increase of the VTE temperature to 1200 °C, 1250 °C, and 1300 °C increases the diffusion rates and the surface concentration decreases to 49.3 mol%, 49.1 mol% and 48.5 mol%, followed by the smaller concentration gradients, respectively.

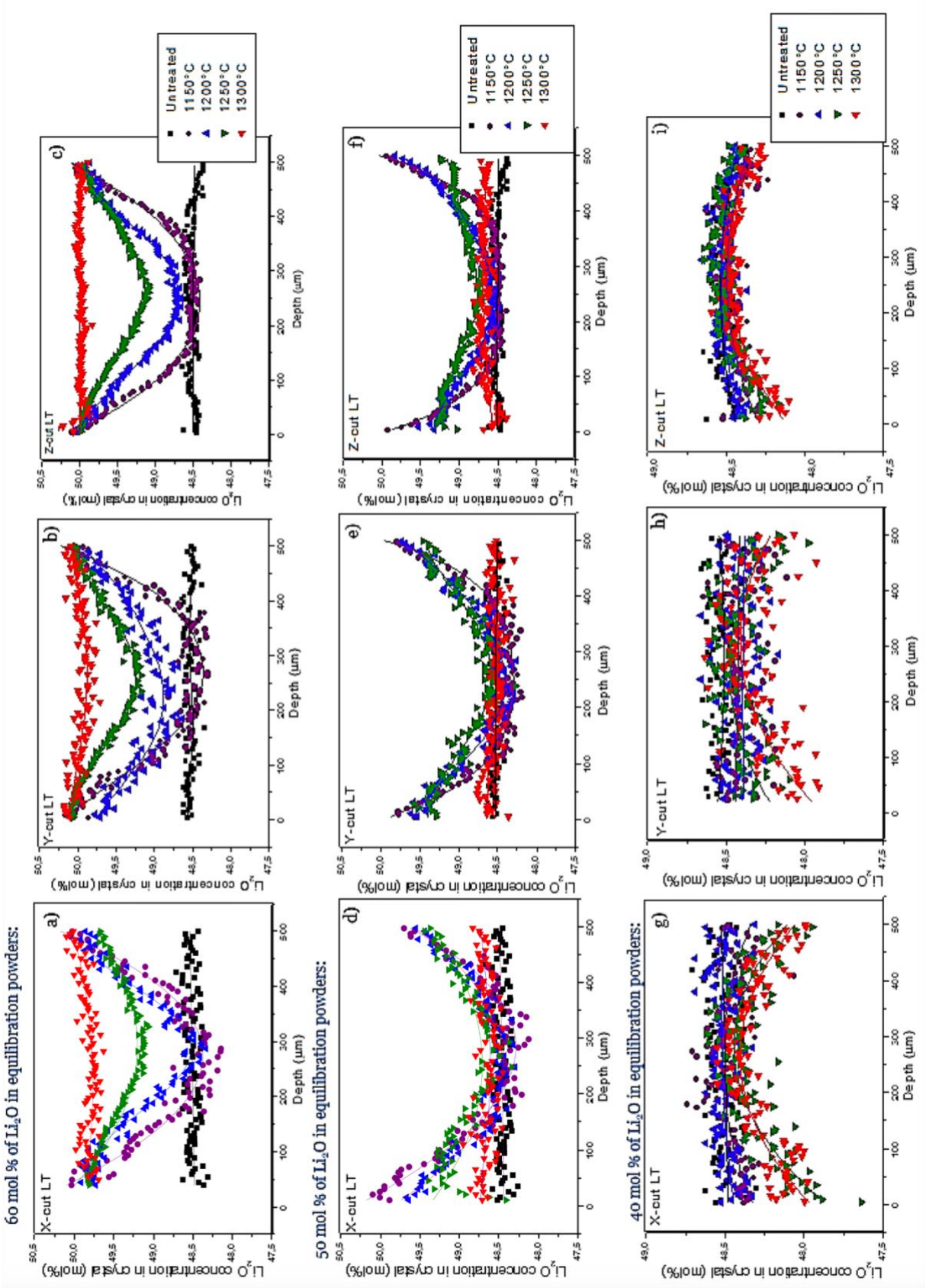

Figure 4. Li_2O concentration profile (measured by means of Raman spectroscopy, for more details see text) across the thickness of X-, Y- and Z-cut LT crystals, treated by VTE at different temperatures (1150 – 1300 °C) for 10h using equilibration powders with 60 mol%, 50 mol% and 40 mol% of Li_2O. The profiles of untreated crystals are given for comparison.

Table 2. The ΔC_{Li2O} (difference between Li_2O concentration on the crystal surface and in the middle of the thickness – depth of 250 μm, **Equation 10**) , $\bar{C}$ (average Li_2O concentration across the crystal thickness of 500 μm), and C_s (concentration on the crystal surface) of X-, Y-, and Z-cut LT crystals (initially with congruent composition containing 48.5 mol% of Li_2O) treated by VTE at 1150 °C – 1300 °C for 10h using Li-poor powders (40 mol% of Li_2O), LT stoichiometric powders (50 mol% of Li_2O), and Li-rich powders (60 mol% of Li_2O).

T (°C)	X_{Li2O} in equilibration powders (mol %)								
	40	50	60	40	50	60	40	50	60
	$\bar{C}$ in crystal (mol%)			ΔC_{Li2O} in crystal (mol %)			C_s in crystal (mol %)		
X-cut	(± 0.15 mol%)						(± 0.05 mol%)		
1150	48.44	48.78	48.96	0.18	1.76[a]	1.94[a]	48.50	49.62	49.87
1200	48.5	48.91	49.26	0.07	1.26	1.26	48.61	49.26	49.79
1250	48.48	48.97	49.85	0.42	0.6	0.45	48.24	49.10	49.89
1300	48.39	48.71	49.99	0.54	0.11	0.09	48.16	48.55	49.93
Y-cut	(± 0.11 mol%)						(±0.05 mol%)		
1150	48.38	48.70	49.01	0.02	1.57[a]	1.64[a]	48.51	49.43	49.88
1200	48.43	48.88	49.23	0.06	1.15	0.86	48.52	49.34	49.92
1250	48.37	48.96	49.69	0.25	0.81	0.68	48.33	49.05	49.93
1300	48.28	48.54	49.98	0.43	0.1	0.12	48.10	48.42	50.00
Z-cut	(± 0.06 mol%)						(± 0.14 mol%)		
1150	48.44	48.78	48.96	0.18	1.49	1.59 [a]	48.37	49.66	49.88
1200	48.50	48.91	49.26	0.12	0.77	1.27	48.40	49.49	49.88
1250	48.48	48.97	49.86	0.28	0.39	0.34	47.85	49.20	49.83
1300	48.39	48.66	49.99	0.34	0.14	0.01	47.90	48.39	49.92

[a] ΔC_{Li2O} should be 1.5 as these crystals were twinned and the Raman dampings were affected by presence of oblique modes.

Li_2O-poor equilibration powders are supposed to serve as an Li_2O sink and to accelerate the loss of Li_2O from the treated crystals. However, the change of Li concentration remains small (0.1 - 0.2 mol%), and the compositions of treated crystals are close to the congruent one (Figure 4, Table 2). The induced gradients by these treatments were considerably smaller than those obtained by using stoichiometric LN or Li-rich powders at the same temperatures. The strongest gradient was attained by the treatment at 1300 °C and the change of the concentration was observed up to the depth of approximately 100 μm. The average Li_2O concentration across the thickness ($\bar{C}$) in the crystals treated using Li-poor powders in the temperatures of 1150 °C - 1300 °C ranged from 48.5 mol% to 48.28 mol%. These results are consistent with the observed decrease of the Li_2O loss with the increase of nonstoichiometry of $Li_{1-x}Ta_{1+x}O_{3+2x}$ phase (Figure 3). This indicates that very long VTE times are needed for the out-diffusion treatments. For example, Bordui et al. have used 400h long treatments with Li-poor powder at 1100 °C for LN crystals [5].

The diffusivity in each cut of LT was estimated according to the second Fick's law:

$$\frac{\partial C}{\partial t}(x,t) = \frac{\partial}{\partial x}(D\frac{\partial C}{\partial x}), \quad (11)$$

Where C is the concentration in the crystal, which is dependent on depth position in crystal, x, time, t, and D_c is the concentration dependent Li-diffusion coefficient. We approximate that:

- At t = 0 the crystal initial concentration, C_0, is homogeneous and congruent one (C = C_0 = 48.5 mol% at $0 \leq x \leq L$, where L is the thickness of the crystal (L = 500 μm) ;
- The surface concentration C = C_s (at x = 0) is constant (saturated, C_s = 50 mol%) while crystal concentration at x, C_x, is a function of time during VTE treatment for t > 0.
- At t = ∞, the final concentration, $C_s = C_x = C_\infty$, of crystal is homogeneous across the thickness and do not change anymore with time.

Applying these boundary conditions and adapting the first approximation solution for diffusion from a sheet with finite thickness**,** proposed by D.W. Readey [44], to VTE case, the solution of **Equation 11** can be written as

$$C_x = C_\infty - (C_\infty - C_0)e^{-\frac{\pi^2}{L^2}Dt}\sin(\frac{\pi x}{L}), \quad (12)$$

and accordingly, the diffusion coefficient D can be expressed as

$$D = -\frac{L^2}{\pi^2 t}\ln(\frac{C_\infty - C_x}{(C_\infty - C_0)\sin(\frac{\pi x}{L})}). \quad (13)$$

According to Figure 4, the surface concentration is constant only during the treatments using Li-rich (X_{Li2O} = 60 mol%) equilibration powders as the surface is saturated to the stoichiometric composition. Thus, diffusion coefficients as a function of temperature and the treated crystal orientation were estimated only in the case of the VTE treatments using with 60 mol% of Li_2O. It is important to note that this approximation is valid for diffused concentration profiles which can be described by the single sin function. Thus, the concentration profiles treated at 1150 °C for 10h were not considered for Z- and X-cut LT, as well.

The coefficient of self-diffusion of Li_2O, D, was estimated from the **Equation 13** for X-, Y-, and Z-cuts of LT crystals treated by VTE for 10h at 1200 - 1300 °C by using equilibration powder with X_{Li2O} = 60 mol% (**Figure 5**). The diffusion coefficients at 1250 °C were found to be 6.4×10^{-13} m^2/s, 7.1×10^{-13} m^2/s and 6.0×10^{-13} m^2/S along X-, Y- and Z-axes, respectively. The Li self-diffusion coefficients in Z-LT were reported to be 2.9×10^{-14} m^2/s at 1100 °C [42] indicating that diffusion is accelerated by a factor of 20 when temperature is increased from 1100 °C to 1250 °C. The diffusion activation energies along these three directions, estimated by plotting lnD=f(1/T) (Figure 5), were 672 ± 95 kJ/(mol.K), 619 ± 55 kJ/(mol.K), and 531 ± 67 kJ/(mol.K), respectively. The difference between the activation energies of Li+ self-diffusion along different axis is in the error limit. Although smaller activation energy of

diffusion along Z-axis than along the X- and Y-axes could be suspected as the shorter times are needed to attain homogeneous composition in Z-axis oriented LT crystals (Figure 4, Table 2). Anisotropic and faster diffusion along the Z direction was reported in literature for LN crystals [34, 38]. The faster diffusion along the polarisation axis can be explained by the –(Ta-Li-Vacancy)$_n$- channels, while X- and Y-directions do not present such direct paths for the diffusion (see the structure projection in **Figure 6**).

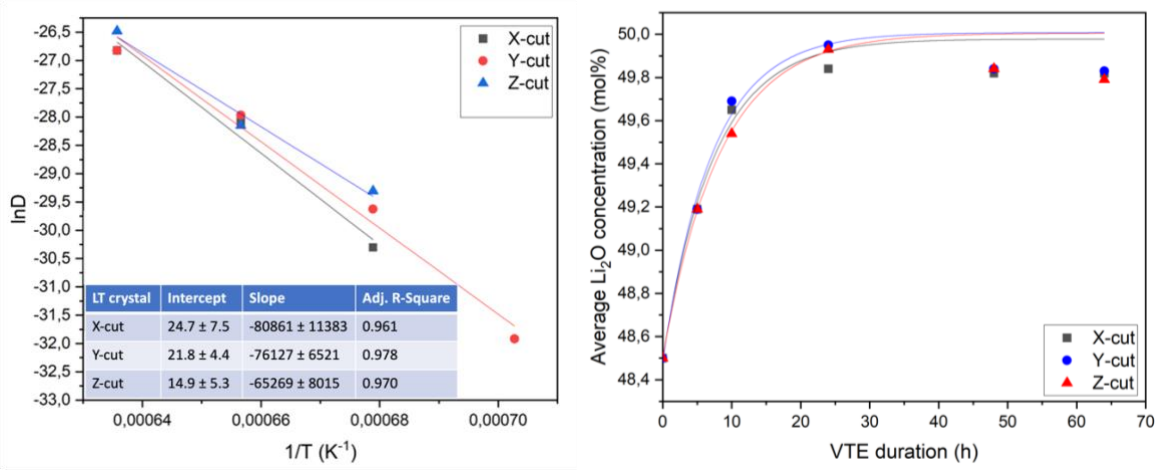

Figure 5. Dependence of Li^+ self-diffusion coefficient along X-, Y- and Z-axes of LT crystals on the VTE temperature, T, in Li-rich atmosphere created by equilibration powder with 60 mol% of Li_2O (left). The lnD dependence on 1/T was fitted by using a linear relationship. The related slopes, intercepts and R-square are indicated in the inset. The average Li_2O concentration, $\bar{c}$, within X-, Y-and Z_LT crystals, treated by VTE at 1250 °C using the equilibration powders with 60 mol% of Li_2O for different durations (right). The duration dependence was fitted by exponential function assuming that the crystal concentration saturates to 50 mol% of Li_2O at $t \geq 48h$.

One can note again that the activation energies along X- and Y-directions are close but with slight difference although they are supposed to be identical for the second rank tensor properties. In the stoichiometric and defect free trigonal crystal structure the diffusion along X- and Y-axes is not aligned to the concentration gradient. In the case of X-cut surface, most of the lithium sites are hindered by oxygen sites and –(Li^+-O^{2-})$_n$- chains are perpendicular to the surface, while in the Y-cut the Li^+ ions containing planes are less hindered by O^{2-} ions. This may explain the difference between diffusion rates in X and Y-cut LT crystals, which was also observed for Ti^{4+} and proton diffusions in LN which also imply Li sites [45-46]. It is also known that defects and impurities highly affect the diffusion process due to Coulomb interactions with diffusing ions and vacancies [47]. The congruent LT crystals, used for VTE, present considerable amount of lattice defects due to nonstoichiometric composition, which are not necessarily equally distributed with respect to the X- and Y-directions (Figure 6) and Li stoichiometry equilibration implies not only Li^+ ion diffusion but also Ta^{5+} ions must move out from antisites. Moreover,

the X- and Y- crystals do not originate from the same boule and X-LT crystals were optical grade while Y-cut LT of SAW grade. In SAW grade crystals there are more impurities and most of the impurities are on Li sites as they are bigger than the Ta ones [45-46].

The volume diffusion rises significantly once the Tammann temperature (1/2 of melting temperature, T_{melt}) is attained and the reasonable diffusion rates can be achieved at temperatures higher than 2/3 of T_{melt} [48]. The self-diffusivity of Li^+ along Z-axis in congruent LN (with 48.38 mol% of Li) was reported to be 0.3 x 10^{-12} m^2/s and in nearly stoichiometric LN (49.85 mol% of Li_2O) - 5 x 10^{-12} m^2/s at $0.88T_{melt}$ [49] indicating that diffusion is highly dependent on the defect concentration/stoichiometry. According to our results in the case of initially congruent LT, the diffusion is of the same order as in nearly stoichiometric LN (3.2 x 10^{-12} m^2/s at $0.79T_{melt}$) although the temperature was more distanced from meting point. According to the linear relationship lnD=f(1/T) (Figure 5), the D = 2.0 x 10^{-10} m^2/s at $0.88T_{melt}$ for LT being two orders higher than that of LN.

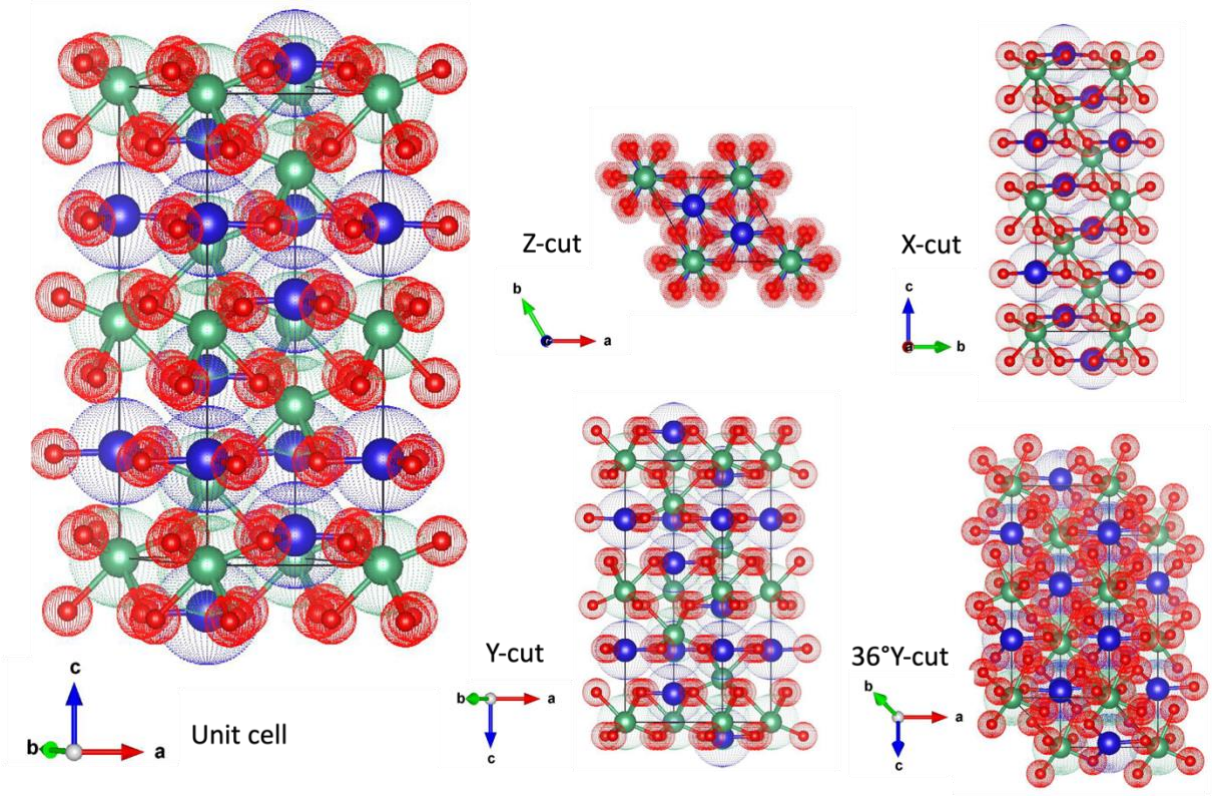

Figure 6. Illustration of LT unit cell and structure projections along X-, Y-, 36°Y- and Z-orientations. The red balls correspond to oxygen ions, green ball- tantalum ions, and blue ones – lithium ions.

2.3. Effect of VTE duration on crystal concentration

In order to investigate the Li^+ concentration gradients as a function of VTE treatment duration and to find out the minimum duration needed to obtain homogenous stoichiometric crystals, X-

, Y-, and Z-cut congruent crystals were treated by VTE using equilibration powder with 60 mol% of Li_2O for duration of 5h, 10h, 24h, 48h and 64h at 1250°C. The Li_2O concentration change across the crystal thickness, estimated by means of Raman spectroscopy, as a function of VTE duration is presented in **Figure 7**. The $\Delta C_{Li2O,}$ $\bar{C}$, and C_s of these samples are summarized in Table 3. In the case of the short treatment durations (5-10h), the crystals present strong composition gradients. After 5h of treatment, the X- and Y- crystals presented the composition still close to the congruent one in the central part of the thickness while the diffusing Li+ ions already diffused to the depth of > 250 μm in the Z-cut LT confirming that Li^+ self-diffusion is faster along Z-axis. The VTE with duration longer than 24h is needed to attain nearly stoichiometric composition homogeneous composition across the thickness in all studied crystal cuts. The crystals treated for 48h and 64h presented homogeneous composition across the thickness.

Once the homogeneous stoichiometric composition is attained, longer diffusion times are supposed as well to results in the homogeneous stoichiometric composition across the thickness if the equilibration powders continue to supply constant partial vapor pressure of Li_2O as Li-rich phases do not form from LT phase during VTE process and the saturated composition corresponds to the stoichiometric one. In the case of the VTE treatment at 1250 °C using equilibration powder with 60 mol% of Li_2O, the average concentration of the LT crystals, $\bar{C}$, as a function of treatment duration, t, can be represented by exponential function (Figure 5 right):

$$\bar{C} = (50.00 \pm 0.04) - (1.5 \pm 0.08)e^{-(0.14\pm0.02)t}. \quad (14)$$

The difference between different cuts is within the experimental errors indicated in the **Equation 14**. According to Equation 14, homogeneous 49.99 mol% concentration can be attained by treatment of 36h. It is important to note that we have observed that the crystals treated for 48h or 64h became slightly more deficient in Li_2O than the stoichiometric composition (Table 3) indicating that the equilibration powders were losing their Li_2O vapor delivery efficiency during long treatments. This issue must be considered in the VTE treatments using ceramic crucibles although they are closed with cover. To overcome this issue and to make the fabrication of crystals with controlled homogeneous composition less duration dependent, the amount off the treatment powders must be increased. It should be noted that temperatures lower than 1250 °C (0.76 T_{melt}) need longer duration for obtaining homogenous crystals. This agrees with results reported by P.F. Bordui et al.[5], in their work, the VTE of LT carried out by using Li-rich powders, at 1100°C (0.67T_{melt}), requires a minimum of 60h. Z. Wang et. al found that VTE duration of 20h and 15.6h is needed for congruent LN crystals at

1100 °C (0.88T_{melt}) by using Li-rich powders (68 mol% of Li_2O) to attain the stoichiometric composition on the surface, estimated from the birefringence measurements. However, the studied thickness/depth were not estimated and the homogeneity across the thickness was not studied in this work [38]. It is important to note that according to our results, the Li_2O average concentration of surface layer across 2 μm thickness is around 49.55 mol% after 5h treatment and it reached stoichiometric composition after 24h (Table 3). Further increase of treatment time starts to reduce the surface stoichiometry confirming the continuously changing equilibration powder composition (Figure 3).

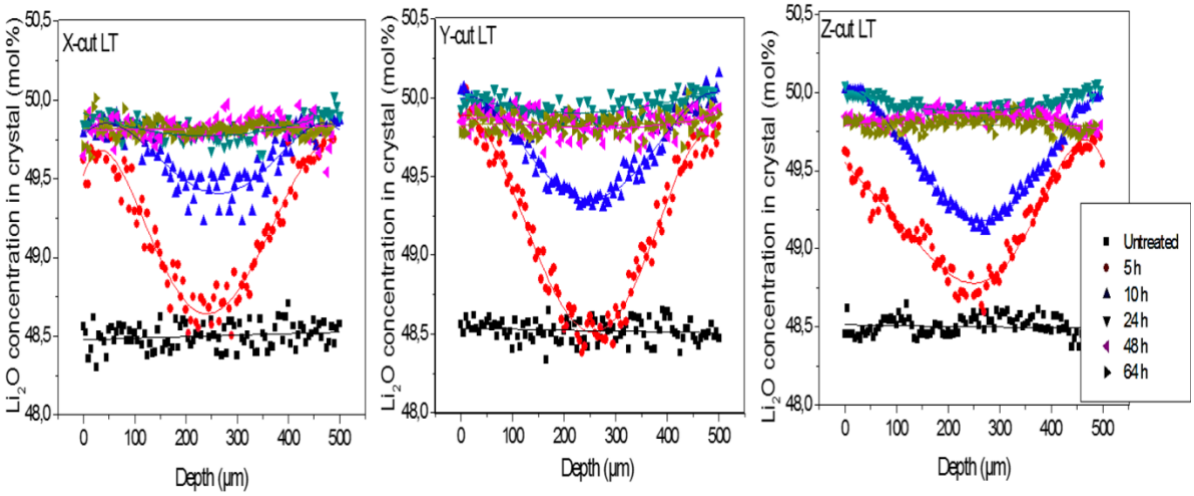

Figure 7. Li_2O concentration profile (measured by means of Raman spectroscopy, for more details see text) across the thickness of X-, Y- and Z-cut LT crystals, treated by VTE at 1250 °C for different durations, ranging from 5h to 64h, using equilibration powders with 60 mol%, of Li_2O. The profiles of untreated crystals are given for comparison.

Table 3. The ΔC_{Li2O} (difference between Li_2O centration on the crystal surface and in the middle of the thickness – depth of 250 μm, **Equation 10**) , $\bar{C}$ (average Li_2O concentration across the crystal thickness of 500 μm), and C_s (concentration on the crystal surface) of X-, Y-, and Z-cut LT crystals (initially with congruent composition containing 48.5 mol% of Li_2O) treated by VTE at 1250 °C for different durations in the range of 5h - 64h using Li-rich powders (60 mol% of Li_2O).

Crystal cut	time (h)	$\bar{C}$ (mol %)	ΔC_{Li2O} (mol %)	Cs (mol %)
		±0.15 mol%		±0.05 mol%
	5	49.19	0.96	49.56
	10	49.65	0.38	49.89
X-cut LT	24	49.84	0.16	49.96
	48	49.82	0.04	49.75
	64	49.82	0.06	49.60
		±0.15 mol%		±0.05 mol%
	5	49.19	1.42	49.54
	10	49.69	0.65	49.92
Y-cut LT	24	49.95	0.15	50

	48	49.84	0.05	-
	64	49.83	0.02	49.68
		±0.06 mol%		±0.10 mol%
	5	49.19	0.93	49.55
	10	49.54	0.86	49.91
Z-cut LT	24	49.93	0.11	49.99
	48	49.84	0.04	49.77
	64	49.79	0.02	49.60

2.4. Effect of equilibration powder composition

In order to fabricate the LT crystals with different compositions varying from sub-congruent to (nearly) stoichiometric composition, the Y-, 36°Y- and Z-cut LT crystals were treated using equilibration powders with Li_2O concentration of 40-60 mol% (100 g of powders were placed in crucible with 115 mm diameter and 22 mm height, Figure 1) at 1250°C for 64 h. Longer treatment times than previously estimated 36h needed for homogenization were used to assure the absence of any composition inhomogeneity, which might induce the twin formation. The rotated LN orientations are frequently used in piezoelectric devices, therefore, the possibility to control the concentration in the rotated 36°Y-cut was studied, as well. Li_2O concentration was homogeneous across the crystal thickness as illustrated for the Y-cut LT crystals treated by stoichiometric LT and Li-rich powders (**Figure 8**).

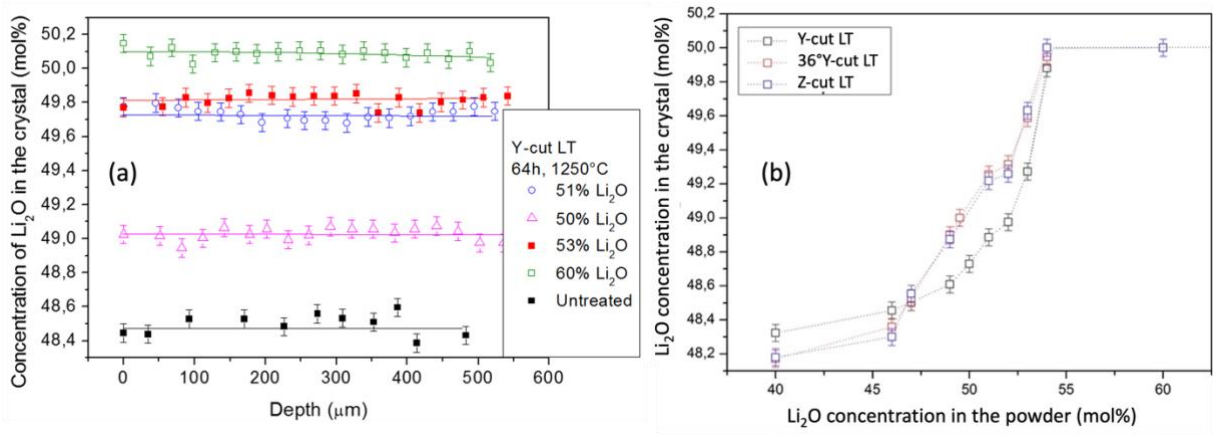

Figure 8. Homogeneity of Li_2O concentration in crystal thickness in Y-cut LT crystals treated by VTE at 1250 °C for 64 h using equilibration powders with different Li content (a). Li_2O concentration in the Y-, 36°Y- and Z-cut LT crystals as a function of equilibration powder concentration used for VTE at 1250°C for 64h (b). The points are connected for the guideline.

The relationship between the crystal concentration and that of the equilibration powders is presented in Figure 8. The Li_2O concentration in crystals is not equal to that of powders and it changes nonlinearly with increasing Li_2O content in powders. Crystals, treated with Li-poor powder (40 mol % of Li_2O) acting as infinite sink of Li_2O [31], present Li_2O content slightly lower than that of untreated congruent crystal (between 48.0 and 48.4 mol%). The crystals,

treated with powders containing Li_2O concentration > 48.5 mol % Li_2O had a higher Li_2O concentration (48.6-50 mol%) than the composition of congruent initial crystal composition (48.5 mol%) but lower than that of the equilibration powder (Figure 8 b). Nearly stoichiometric crystals were attained by using equilibration powders with $X_{Li2O} \geq 54$ mol % at these VTE conditions. As mentioned above, the maximum Li_2O concentration in LT crystals is stoichiometric one (50 mol%). Lithium concentration in treated crystals depends also on the crystallographic cut because the diffusion velocity changes with crystallographic axis, as described above. One can note that the enrichment in Li-rich atmosphere and the decrease in Li-poor atmosphere is slower in X-cut crystals and the obtained final treated X-LT crystal concentration is smaller or higher than those of Z- and 36°Y-LT crystals treated at the same VTE conditions. Z- and 36°Y-LT crystals have presented identical concentrations (within measurement errors) after VTE treatments. In the case of the 36°Y rotated cut, the Li ions are placed exactly above another layer of Li ions (Figure 6), which facilitates the diffusion like in the Z-axis crystals.

4. Concluding remarks

To summarize, the relationship between VTE conditions such as temperature, duration and the composition of the equilibration powder and the composition and its homogeneity of the LT crystals was studied. For this purpose, the Li_2O loss from equilibration powders was determined as a function of treatment temperature and duration and it was shown that the equilibration powder capacity to deliver Li_2O vapor changes continuously their composition with the treatment time. The treated crystal composition on the surface and across the thickness were mapped by means of Raman spectroscopy. In agreement with literature on VTE process on LN crystals, it was found that Li^+ self-diffusion is anisotropic and it is faster along c-axis due to the $–(Nb\text{-}Li\text{-}Vacancy)_n-$ structural channel. This was confirmed by the shorter times needed for the homogenisation of the treated crystal composition across the thickness and higher Li_2O amount obtained in the Z-LT than Y-oriented LT treated at the same conditions. The diffusion coefficients were found by using first approximation solution, considering single sinus function for diffusion concentration profile, of the second Fick law. The diffusion activation energies along X-, Y- and Z-axes were estimated to be 672 ± 95 kJ/(mol.K), 619 ± 55 kJ/(mol.K), and 531 ± 67 kJ/(mol.K), respectively. VTE temperature of 1250 °C was selected as optimal one as it enables relatively fast diffusion and reasonable Li_2O concentration in the powders with treatment time. At this temperature, the homogeneous stoichiometric LT crystals can be obtained by VTE treatment for 36 hours in Li-rich atmosphere, created by powders containing more that 54 mol% of Li_2O. The ability to obtain the homogeneous X-, Y-

, 36°Y- and Z-LT crystals with intermediate compositions between subcongruent composition to stoichiometric one was demonstrated. It is important to note that the out-diffusion of Li_2O oxide from congruent and sub-congruent compositions is very slow. To attain homogeneous composition across the crystal is essential in order to avoid the development of the mechanical stress and consequently crack or mechanical domain formation. As VTE treatment is done above the Curie temperature, the equilibrated LT crystals present ferroelectric polydomain structure and requires electrical poling. In general, the compositions with higher Li content present lower coercive fields (congruent LT – 211 kV/cm and stoichiometric LT – 1.6 kV/cm) and this facilitates the fabrication of the periodically poled structures [16]. The ferroelectric domain structure was studied in our as-treated samples and it was shown that it is highly dependent on the concentration gradients, as domains form during the cooling below the Curie temperature, which varies significantly with the composition (700 °C for stoichiometric composition and 603 °C for congruent one) [50]. Consequently, the depolarizing fields also depend on composition gradients, and it would require to develop different poling strategies. This further motivates usage of the VTE treated crystals with homogeneous composition.

5. Experimental Section/Methods

VTE processing: X-, Y-, 36°Y- and Z-cut wafers of commercially available congruent lithium tantalate (CLT) (containing 48.5%mol of Li_2O) with optical and saw grade quality (supplied by MTI Corporation) were used for the present study. Hereafter (X,Y,Z) is an orthogonal reference system where Z is parallel to the c-axis and X to the a-axis, which is taken perpendicular to the mirror plane of the 3m point group.

Single ($Li_{1-x}Ta_{1+x}O_{3+2x}$) and two-phase [$Li_{0.97}Ta_{1.03}O_{3+2x}$ + $LiTa_3O_8$ (Li-poor)] or $LiTaO_3$ + Li_3TaO_4 (Li-rich)] powders were prepared using Li_2CO_3 (99.9%) and Ta_2O_5 (99.9%) as starting chemicals. To eliminate moisture, the Li_2CO_3 was dried for 16h at 250 °C. Powders with different molar ratio of [Li_2CO_3] / [Ta_2O_5] were prepared by mixing and milling of initial powder mixture and reacting for 120h at 1000°C.

Characterization by Raman spectroscopy: Raman Spectroscopy was used to determine the Li_2O concentration in crystals and powders. The Jobin-Yvon/Horiba LabRam HR spectrometer and S&I Monovista spectrometer with 514 nm line of an Ar^+ ion laser was used in a backscattering geometry. The Raman spectra were fitted with oscillator functions by using the Igor Pro software and a procedure “Unifit” (written by I. Gregora). In order to check the homogeneity of Li content within the crystals, their cross-sections were diced and

polished by using an automatic dicing saw DISCO DAD 320. The cross section were checked by depth scans at intervals of 5 µm.

X-ray diffraction measurements: XRD measurements were performed by using a Bruker D8 Advance diffractometer (Cu $K_{\alpha 1}$ radiation, λ=1.54056Å). Two phase powders were analyzed by XRD and the content of secondary phase was estimated from Rietveld refinement.

Acknowledgements

This work was supported by the French RENATECH network and its FEMTO-ST technological facility, Bourgogne Franche-Comté region, TDK-EPCOS, the French national ANR projects LINKS ANR20-CE08-0025, and the graduate school EUR EIPHI contract ANR-17-EURE-0002.

Received: ((will be filled in by the editorial staff))
Revised: ((will be filled in by the editorial staff))
Published online: ((will be filled in by the editorial staff))

References

[1] C. K. Campbell, *Surface Acoustic Wave Devices for Mobile and Wireless Communications*, 1st edition. San Diego: Academic Press, **1989**.

[2] R. L. Barns and J. R. Carruthers, *J. Appl. Crystallogr*. **1970**, *3 (5)*, 395.

[3] J. R. Carruthers, G. E. Peterson, M. Grasso, and P. M. Bridenbaugh, *J. Appl. Phys.* **1971**, *42 (5)*,1846.

[4] P. F. Bordui, R. G. Norwood, D. H. Jundt, and M. M. Fejer, *J. Appl. Phys.* **1992**, *71 (2)*, 875.

[5] P. F. Bordui, R. G. Norwood, C. D. Bird, and J. T. Carella, *J. Appl. Phys.* **1995**, *78 (7)*, 4647.

[6] J. G. Bergman, A. Ashkin, A. A. Ballman, J. M. Dziedzic, H. J. Levinstein, and R. G. Smith, *Appl. Phys. Lett.* **1968**, *12 (3)*, 92.

[7] T. Volk and M. Wöhlecke, *Lithium Niobate: Defects, Photorefraction and Ferroelectric Switching*. Springer Science & Business Media, **2008**.

[8] Y. Furukawa, K. Kitamura, S. Takekawa, A. Miyamoto, M. Terao, and N. Suda, *Appl. Phys. Lett.* **2000**, *77 (16)*, 2494.

[9] Y. Furukawa, K. Kitamura, A. Alexandrovski, R. K. Route, M. M. Fejer, and G. Foulon, *Appl. Phys. Lett.* **2001**, *78 (14)*, 1970.

[10] M. Jazbinšek, M. Zgonik, S. Takekawa, M. Nakamura, K. Kitamura, and H. Hatano, *Appl. Phys. B*, **2002**, *75 (8)*, 891.

[11] S. Huband, D.S.Keeble, N. Zhang, A.M.Glazer, A. Bartasyte, and P.A.Thomas, *J. Appl. Phys.* **2017**, *121*, 2.

[12] A.M. Glazer, N. Zhang, A. Bartasyte, D.S. Keeble, S. Huband, and P.A. Thomas, J. *Appl. Crystallogr.* **2010**, *43*, 1305.

[13] M. Gonzalez, A. Bartasyte, B. Dulmet, B. Guichardaz, F. Henrot, F. Bassignot, E. Herth, C. Kajiyama, S. Margueron, I. Bleyl, S. Ballandras, and J.M. Brice, *IEEE IUS proceedings*, Taipei, Taiwan, **2015**.

[14] A. Bartasyte, O. Elmazria, M. Gonzalez, L. Bouvot, E. Blampain, and P. Boulet, *ISAF-ECAPD-PFM proceedings*, Aveiro, Portugal, IEEE TUFFC, **2012**.

[15] S. Kim, V. Gopalan, K. Kitamura, and Y. Furukawa, *J. Appl. Phys.* **2001**, *90 (6)*, 2949.

[16] V. Gopalan, T. E. Mitchell, Y. Furukawa, and K. Kitamura, *Appl. Phys. Lett.* **1998**, *72 (16)*, 1981.

[17] L. Tian, V. Gopalan, and L. Galambos, *Appl. Phys. Lett.* **2004**, *85 (19)*, 4445.

[18] C. Bäumer, C. David, A. Tunyagi, K. Betzler, H. Hesse, E. Krätzig, and M. Wöhlecke, *J. Appl. Phys.* **2003**, *93 (5)*, 3102.

[19] C. Bäumer, D. Berben, K. Buse, H. Hesse, and J. Imbrock, *Appl. Phys. Lett.* **2003**, *82 (14)*, 2248.

[20] U. Schlarb, S. Klauer, M. Wesselmann, K. Betzler, and M. Wöhlecke, *Appl. Phys. A* **1993**, *56 (4)*, 311.

[21] A.M. Glazer, N. Zhang, A. Bartasyte, D.S. Keeble, S. Huband, P.A. Thomas, I. Gregora, F. Borodavka, S. Margueron, and J. Hlinka, *J. Appl. Cryst.* **2012**, *45*, 1030-1037.

[22] P. K. Gallagher, H. M. O'Bryan, and C. D. Brandle, *Thermochim. Acta* **1988**, *133*, 1.

[23] A. Bartasyte, A.M. Glazer, F. Wondre, D. Prabhakaran, P.A. Thomas, S. Huband, D.S. Keeble, S. Margueron, *Mater. Chem. Phys.* **2012**, *134*,728.

[24] N. Iyi, K. Kitamura, F. Izumi, J. K. Yamamoto, T. Hayashi, H. Asano, and S. Kimura, *J. Solid State Chem.* **1992**, *101 (2)*, 340.

[25] L. Shi, Y. Kong, W. Yan, J. Sun, S. Chen, L. Zhang, W. Zhang, H. Liu, X. Li, X. Xie, D. Zhao, L. Sun, Z. Wang, J. Xu, and G. Zhang, *Mater. Chem. Phys.* **2006**, 95 (2–3), 229.

[26] Y. Furukawa, K. Kitamura, E. Suzuki, and K. Niwa, *J. Cryst. Growth* **1999**, *197 (4)*, 889.

[27] S. Kumaragurubaran, S. Takekawa, M. Nakamura, and K. Kitamura, *J. Cryst. Growth* **2005**, *285 (1–2)*, 88.

[28] K. Polgár, Á. Péter, L. Kovács, G. Corradi, and Z. Szaller, *J. Cryst. Growth* **1997**, *177 (3–4)*, 211.

[29] G. I. Malovichko, V. G. Grachev, L. P. Yurchenko, V. Y. Proshko, E. P. Kokanyan, and V. T. Gabrielyan, *Phys. Status Solidi A* **1992**, *133 (1)*, K29.

[30] G. I. Malovichko, V. G. Grachev, E. P. Kokanyan, O. F. Schirmer, K. Betzler, B. Gather, F. Jermann, S. Klauer, U. Schlarb, and M. Wöhlecke, *Appl. Phys. A* **1993**, *56 (2)*, 103.

[31] R. L. Holman, P. J. Cressman, and J. F. Revelli, *Appl. Phys. Lett.* **1978**, *32 (5)*, 280.

[32] Y. S. Luh, M. M. Fejer, R. L. Byer, and R. S. Feigelson, *J. Cryst. Growth* **1987**, *85 (1–2)*, 264.

[33] N. Cheng, W. Hua, X. Feng, and H. Ta, *Mater. Sci. Eng. B* **1995**, *33 (2–3)*, 91.

[34] D.-L. Zhang, W.-J. Zhang, Y.-R. Zhuang, and E. Y. B. Pun, *Cryst. Growth Des.* **2007**, *7 (8)*, 1541.

[35] X. Liang, X. Xuewu, C. Tow-Chong, Y. Shaoning, Y. Fengliang, and T. Y. Soon, *J. Cryst. Growth* **2004**, *260 (1–2)*, 143.

[36] D.-L. Zhang, B. Chen, D.-Y. Yu, and E. Y.-B. Pun, *Cryst. Growth Des.* **2013**, *13 (4)*, 1793.

[37] B. Chen, P.-R. Hua, D.-L. Zhang, and E. Y.-B. Pun, *J. Am. Ceram. Soc.* **2012**, *95 (3)*, 1018.

[38] Z. Wang, P.-R. Hua, B. Chen, D.-Y. Yu, E. Y.-B. Pun, and D.-L. Zhang, *J. Am. Ceram. Soc.* **2012**, *95 (5)*, 1661.

[39] D.-L. Zhang, Z. Wang, P.-R. Hua, and E. Y.-B. Pun, *J. Am. Ceram. Soc.* **2012**, *95 (9)*, 2798.

[40] M. Katz, R. K. Route, D. S. Hum, K. R. Parameswaran, G. D. Miller, and M. M. Fejer, *Opt. Lett.* **2004**, *29 (15)*, 1775.

[41] M. Palatnikov, O. Shcherbina, V. Sandler, N. Sidorov, and K. Bormanis, *Ferroelectrics* **2011**, *417 (1)*, 46.

[42] J.M. Ivy and G.L. Brennecka, *Journal of Materials Science* **2022**, 57 (13), 70354.

[43] S. Margueron, A. Bartasyte, A.M. Glazer, E. Simon, J. Hlinka, I. Gregora, and J. Gleize, *J. Appl. Phys.* **2012**, *111*, 104105.

[44] D.W. Readey, *Kinetics in materials science and engineering*, CRC Press, Taylor &Francis group, **2017**.

[45] K. K. Wong, *Properties of Lithium Niobate*, Emis Datareviews Series, 28,The Institution of Engineering and Technology, **2002**.

[46] T. Volk and M. Wöhlecke, *Lithium Niobate_ Defects, Photorefraction and Ferroelectric Switching*, Springer Series in Materials Science 115, Springer-Verl, **2008**.
[47] R. E. Newnham, *Properties of Materials_ Anisotropy, Symmetry, Structure*, Oxford University Press, USA, **2005**.
[48] S. Trolier-Mckinstry and R. Newnham, *Materials Engineering, Bonding, Structure, and Structure-Property Realationships*, Materials Research Society, Cambridge University Press **2018**.
[49] D. H. Jundt, M. M. Fejer, R. G. Norwood, and P. F. Bordui, *J. Appl. Phys.* **1992**, *72 (8)*, 3468.
[50] V.I. Pryakhina, E.D. Greshnyakov, B.I. Lisjikh, A.R. Akhmatkhanov, D.O. Alikin, V.Ya. Shur, and A. Bartasyte, *Ferroelectrics* **2018**, 525(1), 47–53.

Homogeneous X-, Y-, 36°Y- and Z-cut crystals with homogeneous and controlled Li_2O (non)stoichiometry in the composition range of LT phase existence (47 – 50 mol%) are fabricated by means of vapor transport equilibration. Effort is done to optimise the VTE conditions as temperature, duration and equilibration powder composition for controlled fabrication process.

.

Minerva Gonzalez, Samuel Margueron, Tomas Murauskas, Pascal Boulet, Ludovic Gauthier Manuel, Stefania Oliveri, and Ausrine Bartasyte *Corresponding Author*

Influence of parameters in vapour transport equilibration treatment on composition and homogeneity of $LiTaO_3$ single crystals

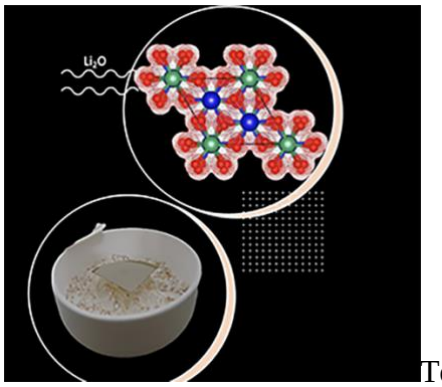

ToC figure (Size: 55 mm broad × 50 mm high)